View Article Online
View Journal

Dalton Transactions

An international journal of inorganic chemistry

Accepted Manuscript

This article can be cited before page numbers have been issued, to do this please use: D. Florio, C. De Simone, A. Annunziata, F. Ruffo, D. Marasco and S. La Manna, *Dalton Trans.*, 2026, DOI: 10.1039/D6DT00454G.

ROYAL SOCIETY OF CHEMISTRY

rsc.li/dalton

View Article Online
DOI: 10.1039/D6DT00454G

ARTICLE

Rational Design of η⁶-Arene Ru(II) Complexes for Amyloid-β Targeting: Influence of Coordination Lability and Aromaticity

Received 00th January 20xx,
Accepted 00th January 20xx

DOI: 10.1039/x0xx00000x

Daniele Florio [1,α], Carla De Simone [2,b], Alfonso Annunziata [c, †], Francesco Ruffo[c], Daniela Marasco [b,*], Sara La Manna [b,*]

The interaction of transition-metal complexes with amyloidogenic peptides represents a promising strategy for controlling pathological protein aggregation through coordination chemistry and supramolecular effects. Herein, we investigate a series of η⁶-arene Ru(II) complexes bearing a glucosylated N-heterocyclic carbene (NHC) ligand and distinct ancillary ligand environments as modulators of amyloid-β ($Aβ_{1–42}$ and $Aβ_{21–40}$) aggregation. By systematically varying the nature of the arene, overall charge, and ligands lability, we elucidate how the design of the complexes governs peptide binding, aggregation pathways, fibril morphology, and cytotoxicity. Thioflavin T fluorescence assay revealed pronounced, peptide-dependent inhibition of amyloid aggregation**. RuPhenCym** strongly suppresses $Aβ_{1–42}$ fibrillization, whereas the neutral, dichloro complex **$RuCl_2Tol$** exhibited enhanced efficacy toward the shorter $Aβ_{21–40}$ fragment. Circular dichroism spectroscopy demonstrated that Ru complexes modulate peptide secondary structure, promoting early β-structured species formation and altering aggregation kinetics. Scanning electron microscopy showed substantial remodeling of fibril morphology, including reduced fiber length and increased heterogeneity, indicative of off-pathway aggregation. Electrospray ionization mass spectrometry provided direct evidence of adducts formation in the presence of **$RuCl_2Tol$**, highlighting the crucial role of labile chloride ligands in generating coordination vacancies that enable peptide binding. Importantly, **$RuCl_2Tol$** and **RuPhenCym** significantly attenuate $Aβ_{1–42}$-induced cytotoxicity in SH-SY5Y neuroblastoma cells without exhibiting intrinsic cellular toxicity. Overall, this study establishes clear structure–activity relationships linking ligand environment, coordination chemistry, and biological outcome in η⁶-arene Ru(II)–amyloid systems. These findings identify glucosylated η⁶-arene Ru(II) complexes as tunable bioinorganic platforms for the selective modulation of amyloid aggregation, providing a rational framework for the development of metal-based agents targeting neurodegenerative disorders..

Introduction

Amyloid-β (Aβ) peptides are generated from amyloid precursor protein (APP) by β- and γ-secretase cleavage. Among them, $Aβ_{1-42}$ is strongly implicated in Alzheimer's disease because it aggregates more readily and forms neurotoxic oligomers and fibrils compared with $Aβ_{1-40}$, a property largely attributed to its hydrophobic C-terminal region [1]. To elucidate sequence determinants of aggregation, shorter Aβ fragments have been widely studied. The $Aβ_{21-40}$ fragment retains most of the hydrophobic C-terminal domain while excluding the N-terminal region involved in metal binding and electrostatic interactions. Experimental studies show that $Aβ_{21-40}$ can self-assemble into amyloid-like fibrils and reproduce key aggregation features of full-length Aβ, making it a useful minimal model for C-terminal-driven amyloid formation and for testing aggregation modulators [2] Complementary studies on the neighboring Aβ $_{21-30}$ segment indicate that this region adopts relatively stable folded conformations that may act as early structural nuclei during peptide folding and aggregation, further supporting the central role of residues 21–40 in amyloid assembly [2-4] . Ruthenium complexes have emerged as promising modulators of amyloid aggregation through a variety of molecular structures and mechanisms. Ru(II) polypyridyl complexes, which often employ bipyridine or phenanthroline ligands, can engage in strong noncovalent interactions with Aβ via π–π stacking and hydrophobic contacts [5], and in some cases chelate redox-active metal ions as Cu(II) which are associated with Aβ plaques [6]. A series of Ru(II) polypyridyl compounds bearing a hydrophobic ancillary ligand (tetra-xylene bipyridine glycoluril, txbg) showed nearly complete inhibition of Aβ aggregation at micromolar concentrations and low toxicity in neuroblastoma cells [7]. "Piano-

[a.] *IRCSS SYNLAB SDN, Via G. Ferraris 144, Naples 80146, Italy.*
[b.] *Department of Pharmacy, University of Naples Federico II, 80131, Naples, Italy.*
[c] *Department of Chemical Sciences, University of Naples Federico II, 80126, Naples, Italy.* [α]*co-first,* [†]*present address: IMDEA Nanociencia, C. Faraday, 9, Fuencarral-El Pardo, 28049 Madrid.*
* Corresponding author: Daniela Marasco; E-mail: daniela.marasco@unina.it; Sara La Manna sara.lamanna@unina.it

Electronic Supplementary Information (ESI) available: Figure S1 ThT-fluorescence assay of Ru complexes alone at 100 µM., Figure S2. ESI-MS spectra of the Aβ $_{21–40}$ peptide in the absence (A) and presence of RuBipyCym (B) and RuPhenCym (C). The peaks marked with bn derive from spontaneous source fragmentation of Aβ $_{21–40}$. Figure S4. MTT assay of Ru complexes at t = 0 , 2 and 24 h, Table S1: t ½ and maximum intensity values related to ThT experiments, Table S2, S3: Deconvolution of CD spectra reported in Figure 3, Table S4: Experimental m/z values detected in the spectra of $Aβ_{21-40}$ and $Aβ_{1-42}$ alone and with the addition of RuBipyCym. Table S5: Experimental m/z values detected in the spectra of Aβ21-40 and Aβ1-42 alone and with the addition of RuPhenCym See DOI: 10.1039/x0xx00000x

stool" Ru(II) arene complexes also demonstrated potent anti-amyloid activity: two Ru(II) complexes of the form [Ru(*p*-cymene)Cl(L) (L= bidentate nitrogen ligand) inhibited aggregation of $A\beta_{1-42}$ and the most active compound protected neuronal cells (Neuro-2a) and computational docking suggested both hydrophobic interactions and coordination to peptide binding sites [8]. More recently, a series of Ru(II)–arene azole complexes was shown to be exceptionally stable in aqueous environments, to coordinate to Aβ, and to strongly inhibit aggregation, with one compound ("RuBO") also reducing cytotoxicity [9]. Another important approach involves photoactivatable Ru(II) polypyridyl complexes: in one study, distorted Ru(II) complexes bearing sterically encumbered bipyridine ligands were irradiated, triggering the loss of one ligand and generating coordinatively unsaturated species capable of binding histidine residues in Aβ. This ligand loss caused a rapid change in aggregation behavior, redirecting Aβ into large, amorphous, insoluble aggregates rather than typical fibrils and these off-pathway species were shown to be more susceptible to proteolytic degradation[10]. In a more recent study, two Ru(II) polypyridyl complexes with extended planar phenanthroline ligands were engineered to pre-associate with Aβ via hydrophobic interactions, and, upon photoactivation, release ligands that promote peptide binding and scavenge Cu–Aβ species, thereby reducing redox cycling and reactive oxygen species (ROS) production. [11] In addition to ligand-exchange systems, Ru(II) complexes that release biologically active small molecules under light have also been explored. For instance, CO-releasing Ru(II) compounds with benzimidazole and terpyridine moieties modulate the aggregation of model amyloidogenic peptides via the formation of adducts after loss of labile ligands on irradiation. [12]

Mechanistically, the effects of Ru complexes derive from a combination of noncovalent binding (hydrophobic and π–π), coordination to peptide residues (especially His), displacement or sequestration of metal ions like Cu(II), and, in photoactivatable systems, ligand release or ROS / singlet oxygen generation [13 6 14]. Indeed, at the molecular level, these complexes coordinate to the imidazole side chains of His within N-terminal portion of Aβ, serving as critical metal-binding sites influencing peptide conformational dynamics. This coordination interferes with the ability of Aβ to adopt the β-sheet-rich structures necessary for nucleation and fibril elongation. Beyond histidine coordination, ruthenium complexes engage in hydrophobic/aromatic interactions facilitated by their aromatic ligands, thus destabilizing the hydrophobic core that promotes amyloid assembly [10, 15, 16]. They also form hydrogen bonds through amine ligands, further stabilizing non-fibrillar peptide conformations.

In several previous studies, we examined the effects of two η^6-arene glucosylated Ru(II) complexes on the self-aggregation of several amyloidogenic peptides with different sequences and aggregation kinetics. These complexes contain two chloride ligands, a glucosylated N-heterocyclic carbene (NHC), and different arene ligands, Their activity was tested on small amyloid models, including the $NPM1_{264-277}$ fragment of nucleophosmin-1 [17-19], the BSP_{27-32} fragment of the human Bloom syndrome protein [20], and the β2-microglobulin fragment $\beta2m_{83-88}$ derived from proteolytic cleavage [21, 22]. In the present study, for the first time, we investigated three additional Ru(II) complexes—**$RuCl_2Tol$**, **RuBipyCym,** and **RuPhenCym** (Figure 1), for their ability to modulate the self-aggregation of $A\beta_{1-42}$ and $A\beta_{21-40}$ peptides.

All three compounds exhibit a piano-stool geometry and contain an NHC ligand bearing a peracetylated β-D-glucose moiety bound through the anomeric nitrogen. **$RuCl_2Tol$** is a neutral complex featuring toluene as the arene ligand quite similar to those already investigated toward small, and His-rich amyloid peptides [17, 22], while **RuBipyCym** and **RuPhenCym** are cationic p-cymene complexes incorporating either 2,2'-bipyridine or 1,10-phenanthroline as chelating ligands, with trifluoromethanesulfonate as the counterion. In them bipyridine and phenanthroline ligands in place of chlorides (Figure 1) are predicted to have a reduced ability as leaving ligands in ligand exchange reactions since in both cases it requires chelate opening.

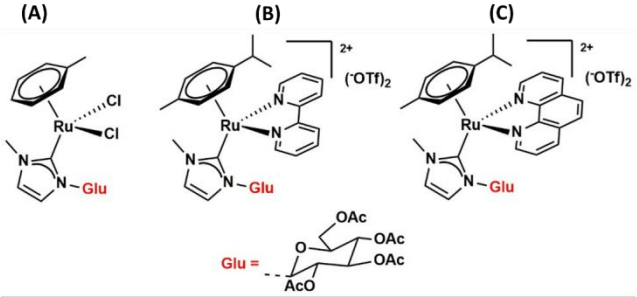

(D)

Peptide	Sequence
$A\beta_{1-42}$	DAEFRHDSGYEVHHQKLVFFAEDVGSNKGAIIGLMVGGVVIA
$A\beta_{21-40}$	AEDVGSNKGAIIGLMVGGVVIA

Figure 1. Schematic structure of (A) **$RuCl_2Tol$**, (B) **RuBipyCym** and (C) **RuPhenCym** Ru compounds. (D) Sequences of amyloid peptides investigated in this study

The investigations were conducted using a broad set of spectroscopic and biophysical methods. Initially, the effects of Ru complexes on ThT fluorescence emission were examined for both amyloids. CD spectroscopy was used to evaluate changes in peptide conformational preferences, while SEM analysis provided insight into the structural impact of Ru complexes on amyloid fibers. ESI-MS was then employed to investigate adduct formation between the amyloid peptides and Ru complexes and viability cellular assays in SH-SY5Y cells allowed to evaluate different effects on typical amyloid cytotoxicity.

Results and discussion

Effects of η^6-Arene Ru(II) Complexes on Amyloid Aggregation

Thioflavin T (ThT) assay was performed to evaluate the effects of Ru complexes on the aggregation kinetics of $A\beta_{1-42}$ and $A\beta_{21-40}$ peptides, at different ratios, (Figure 2): Maximum fluorescence intensities and half-times of aggregation ($t_1/_2$) are reported in Table S1, however, ThT intensity should be interpreted cautiously, as it reflects dye binding to β-structured aggregates rather than a direct quantitative measure of fibrils concentration. As expected, $A\beta_{1-42}$ rapidly aggregated (Figure 2A) as shown by a short lag phase and a steep increase in ThT signal (maximum fluorescence of 200.6 a.u. with a $t_1/_2$ of 95 min). Among the Ru complexes, **RuPhenCym** exhibited the strongest inhibitory effect, reducing the ThT signal (18.2 a.u.), and, at 1:1 ratio, completely hampered the evaluation of $t_1/_2$, while **RuBipyCym** showed minimal effect at 1:0.5 and only partial inhibition at 1:1 ratios (94.6 a.u., $t_1/_2$ = 169 min). **$RuCl_2Tol$** displayed an intermediate efficacy between **RuBipyCym** and **RuPhenCym** activity (135.2 a.u. at 1:0.5 and 40.5 a.u. at 1:1 ratios).

$A\beta_{21-40}$ aggregates more slowly than $A\beta_{1-42}$ ($t_1/_2$ = 286 min) (Figure 2B). Its aggregation was affected by the presence of both **RuBipyCym** and **RuPhenCym**: **RuBipyCym** showed minimal inhibitory activity, while **RuPhenCym** was effective mainly at the 1:1 and less at 1:0.5 ratios, with the overall inhibition weaker than for $A\beta_{1-42}$. Interestingly, **$RuCl_2Tol$** exhibited the strongest effect, with substantial reduction of maximum fluorescence already at 1:0.5 (51 a.u.) and an almost complete suppression at 1:1 ratio (40 a.u.).

These observations suggest a peptide-dependent mechanism of inhibition: indeed, the greater effect of **RuPhenCym** toward $A\beta_{1-42}$ may arise from the presence of extended aromatic interactions between the η^6-coordinated arene and the planar N^N aromatic chelating ligands, with aromatic residues present in $A\beta_{1-42}$ (e.g., His [6, 13] and [14], Tyr [10], and Phe [4, 19, 20]) absent in $A\beta_{21-40}$. In contrast, **$RuCl_2Tol$**, which bears labile chlorides, resulted more effective against the shorter $A\beta_{21-40}$ peptide, likely due to its increased accessibility toward the smaller and more flexible sequence. None of Ru complexes alone exhibited significant signals in this assay (Figure S1).

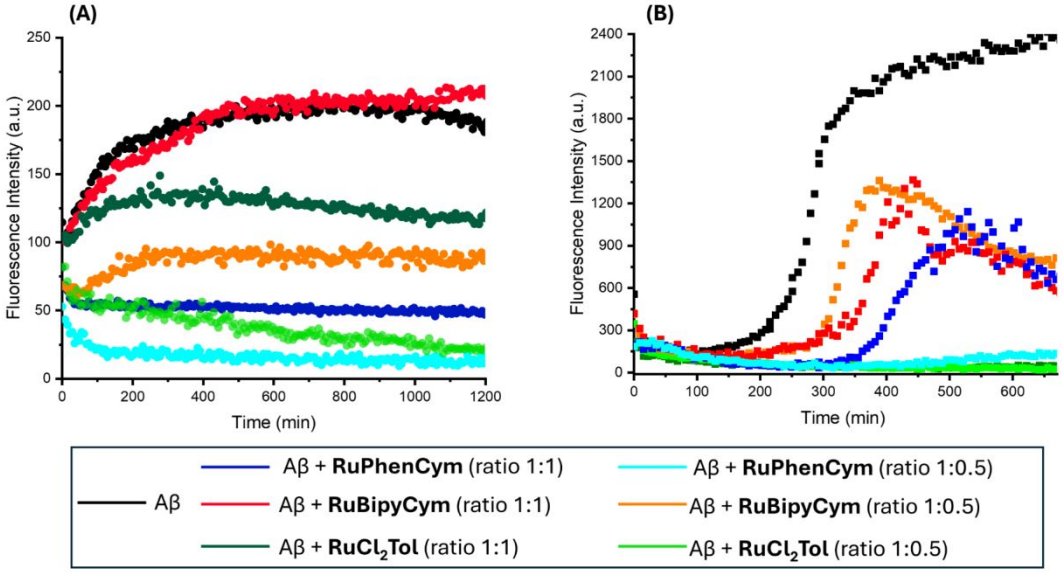

Figure 2. Aggregation kinetics monitored by ThT-fluorescence of (A) $A\beta_{1-42}$ (50 μM), (B) $A\beta_{21-40}$ (100 μM) alone and in the presence of Ru-complexes 1:1 and 1:0.5 peptide: complex molar ratio

.

Conformational Effects of η^6-Arene Ru(II) Complexes on Amyloid Peptides

To investigate the conformational effects of the Ru-complexes on Aβ peptides, CD experiments were performed at a 1:1 peptide-to-complex ratio (Figure 3). At t = 0 the observed β-content (Table S3) likely reflects rapid re-aggregation $A\beta_{1-42}$ alone in PBS[23], and, during time, we observed a complete transition toward β-sheet structure (Figure 3A) [24]. The presence of all three Ru-complexes promoted early β-structured species formation already at t=0, with **RuPhenCym** showing the most pronounced effect over time (Figure 3D). This is supported by CD deconvolution, which indicates a β-content of 40% with **RuPhenCym** (Table S2) at t= 0, reaching 50% after 48 h. A similar but slower effect was observed in the presence of **RuBipyCym** (Figure 3C). For $A\beta_{21-40}$ alone spectra suggested a predominant random coil content (Figure 3E) and **$RuCl_2Tol$** and **RuBipyCym** exhibited minimal effects, with a β-content (Table S3) similar to that of the peptide alone, and a progressive reduction of the Cotton effect over time, but no clear β-sheet transition. Interestingly, since t= 0, in the presence of **RuBipyCym** and

View Article Online
DOI: 10.1039/D6DT00454G

RuPhenCym complexes, an additional positive band at λ 250 nm (Figure 3 G, H) is observed, suggesting a different solvent exposure of the aromatic ligands of the complexes, indicating the formation of adducts with the peptide. In addition, the presence of **RuPhenCym** increased the β-content already at t= 0 (38.5%) (Table S3) and, after 48 h, a more defined β-structure was observed. However, CD spectroscopy cannot distinguish between non-toxic and toxic β-sheet–containing species, including oligomers and these species may correspond to either on-pathway intermediates or off-pathway aggregates, and their precise nature remains to be established.

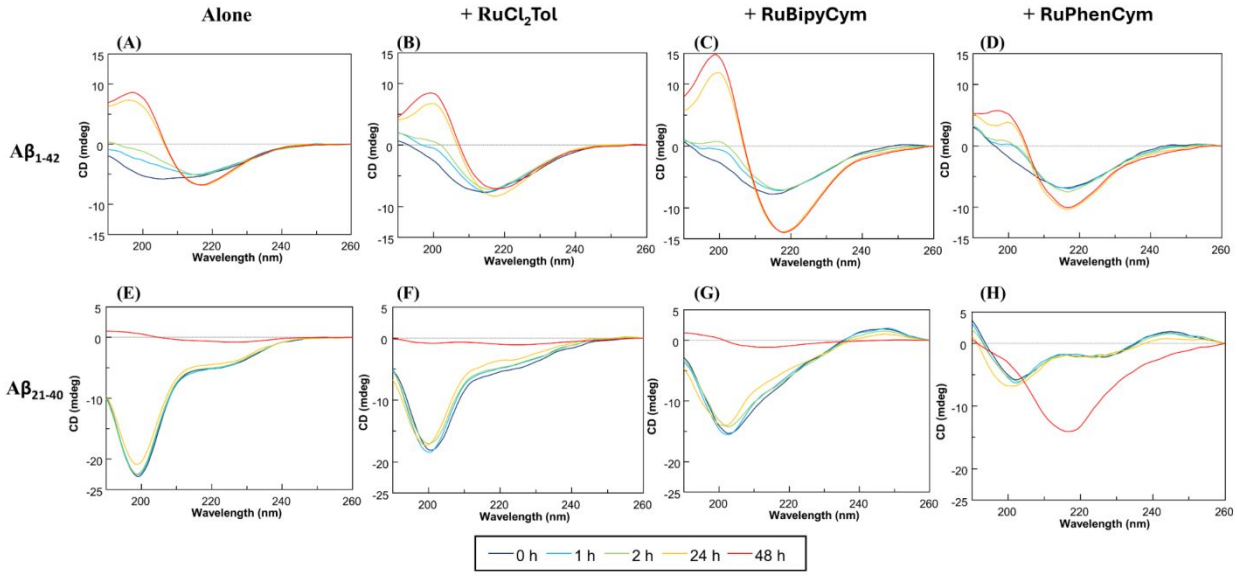

Figure 3. Overlays of CD spectra of (A-D) $A\beta_{1-42}$, (E-H) $A\beta_{21-40}$ peptides in the absence and presence of Ru complexes, subtracted by spectra of complexes alone. All samples were prepared at 1:1 Aβ:Ru molar ratio.

Effects of η⁶-Arene Ru(II) Complexes on Fibril Morphologies

To assess morphological changes in aggregates derived from $A\beta_{1-42}$ and $A\beta_{21-40}$ peptides in the absence and presence of Ru-complexes, scanning electron microscopy (SEM) was employed. Samples were prepared by mixing peptides and complexes at a 1:1 molar ratio and analyzed after 6 h of stirring. Representative micrographs are shown in Figure 4. $A\beta_{1-42}$ alone formed long, well-defined fibers (Figure 4A, A', Table 1), whereas $A\beta_{21-40}$ fibers were shorter and thicker, (Figure 4E, E', Table 1), in line with already reported data [25, 26]. The presence of Ru-complexes altered the morphology of the fibers with distinct fiber populations and heterogeneous lengths and diameters. In the presence of **$RuCl_2Tol$**, $A\beta_{1-42}$ fibers were relatively uniform, slightly thicker than those of the peptide alone (Figure 4B, B', Table 1). In the presence of **RuBipyCym**, fibers were shorter (Figure 4C, C', Table 1), while diameters remained similar to those observed with **$RuCl_2Tol$**. The presence of **RuPhenCym** induced a more heterogeneous morphology, giving rise to three aggregates that differ in both length (in the range of 660–1050 µm) and diameter (in the range of 8–17 µm) (Figure 4D, D', Table 1).

For $A\beta_{21-40}$, the addition of Ru-complexes strongly reduced fiber size, resulting in a single fiber population, in contrast to the multiple populations observed for $A\beta_{1-42}$. In the presence of **$RuCl_2Tol$**, fibers became very short and thin (Figure 4C, C', Table 1), whereas **RuBipyCym** (Figure 4G, G') and **RuPhenCym** (Figure 4H, H') led to slightly longer fibers with diameters of 12–14 µm (Table 1). The Ru complexes alone did not show any fiber formation (data not shown). Granular features observed in some micrographs are attributed to buffer salt residues (figure S5).

View Article Online
DOI: 10.1039/D6DT00454G

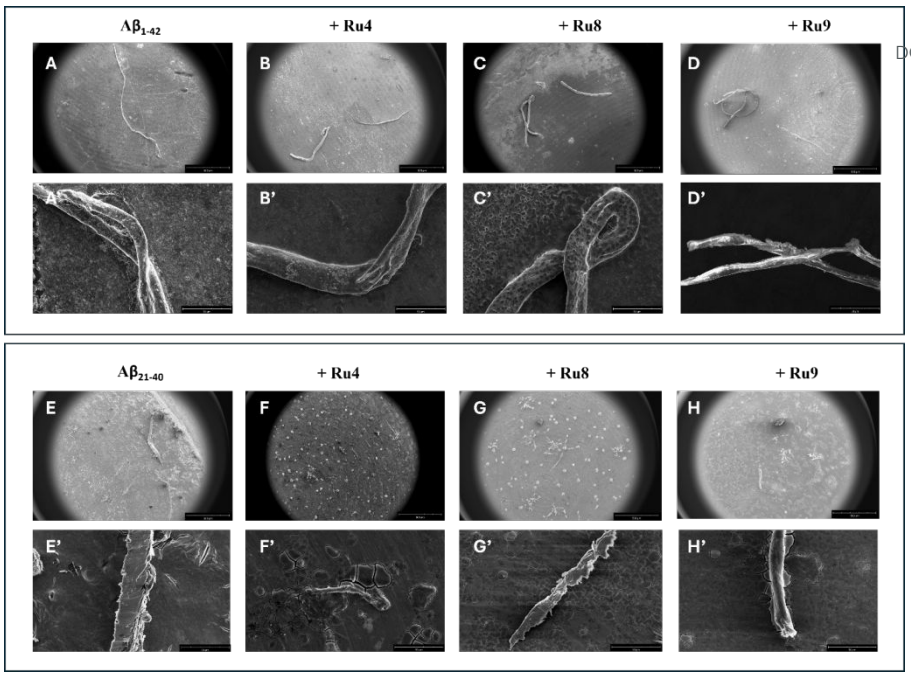

Figure 4. SEM images of, upper panel, $A\beta_{1-42}$ alone (A, A') and in the presence of **$RuCl_2Tol$** (B, B'), **RuBipyCym** (C, C') and **RuPhenCym** (D, D') at a magnification of 220× (A-D) and 2500× (A'-D'); lower panel, of $A\beta_{21-40}$ alone (E, E') and in the presence of **$RuCl_2Tol$** (F, F'), **RuBipyCym** (G, G') and **RuPhenCym** (H, H') at a magnification of 220× (E-H) and 2500× (E'-H').

Table 1: SEM analyses: average diameter and length of fibers obtained for $A\beta_{1-42}$ and $A\beta_{21-40}$ peptides in the absence and presence of Ru complexes

	Average length (µm)	Average diameter (µm)
$A\beta_{1-42}$	1721±3	12±2
$A\beta_{1-42}$: **$RuCl_2Tol$** 1:1	Fiber 1 675 ±4 Fiber 2 801±2	Fiber 1 15±2 Fiber 2 13±2
$A\beta_{1-42}$: **RuBipyCym** 1:1	Fiber 1 1076 ±4 Fiber 2 610±3	Fiber 1 15±2 Fiber 2 13±2
$A\beta_{1-42}$: **RuPhenCym** 1:1	Fiber 1 1052±2 Fiber 2 927±2 Fiber 3 662±4	Fiber 1 8±2 Fiber 2 8±2 Fiber 3 17±2
$A\beta_{21-40}$	665±4	42±3

View Article Online
DOI: 10.1039/D6DT00454G

$A\beta_{1-42}$: **$RuCl_2Tol$** 1:1	83±2	5±2
$A\beta_{1-42}$: **RuBipyCym** 1:1	252±3	12±2
$A\beta_{1-42}$: **RuPhenCym** 1:1	227±4	14±2

ESI-MS Analysis: Formation of η⁶-Arene Ru(II) Complex–Peptide Adducts

To evaluate the formation of direct adducts between Aβ peptides and Ru complexes, they were separately incubated at a 1:1 molar ratio (Aβ:Ru) and analyzed after two hours by electrospray ionization-mass spectrometry (ESI-MS). Figures 5 and 6 show the analysis of each peptide in the presence of **$RuCl_2Tol$.**

The incubation of $A\beta_{1-42}$ with **$RuCl_2Tol$** produced a peak at m/z 1680.21 a.m.u., indicating a stable adduct formed by the peptide and **$RuCl_2Tol$** with the loss of two chlorides ligands and of two acetyl ligands from the sugar portion (Figure 5, Table 2). The tendency to lose acetyl fragment in ESI-MS experimental conditions was already reported for this class of compounds [27]. This evidence suggested that the longer peptide, $A\beta_{1-42}$, may provide multiple donor sites for **$RuCl_2Tol$**. Similar experiments with **RuBipyCym** or **RuPhenCym**, exhibited novel peaks due to the formation of nonspecific associations with trifluoromethanesulfonate ($CF_3SO_3^-$) ions (Figures S2, S3 and Tables S4, S5). The lack of stable peptide adducts with **RuBipyCym** and **RuPhenCym** can be explained by the presence of the bidentate ligands in their coordination spheres, that do not undergo ligand exchange the ruthenium center, hampering peptide coordination at the metal center and detection of the relative adducts.

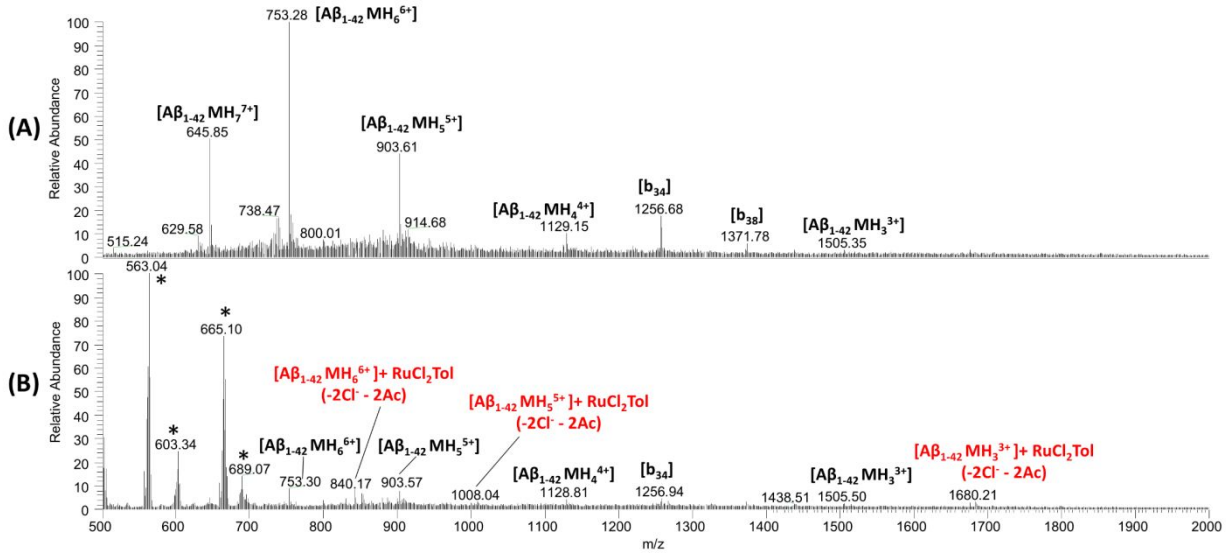

Figure 5. ESI-MS spectra of the $A\beta_{1-42}$ peptide in the absence (A) and presence of **$RuCl_2Tol$** (B). The peaks marked with bn derive from spontaneous source fragmentation of $A\beta_{1-42}$ (b series elements). Asterisks (*) highlight the species present in the control (**$RuCl_2Tol$** alone)..

In the case of $A\beta_{21-40}$ (Figure 6), signals of the b-series were generated from spontaneous in-source fragmentation events, as previously reported [28]. The presence of **$RuCl_2Tol$** led to the appearance of a distinct peak at m/z 1225.15 a.m.u. (Table 2), corresponding to the peptide bound to **$RuCl_2Tol$** complex upon the loss of two chloride ligands and one acetyl group. In the absence of N-terminal histidine residues, coordination may involve side chains such as Glu[22] and Asp[23]. These interactions, combined with the increased flexibility of the shorter peptide, may facilitate coordination to $RuCl_2Tol$ following chloride dissociation. In the presence of **RuBipyCym** or **RuPhenCym** no similar adducts were detected (Figures S2, S3 and Tables S4, S5), while novel signals are consistent with nonspecific adducts involving trifluormethanesulfonate ions.

View Article Online
DOI: 10.1039/D6DT00454G

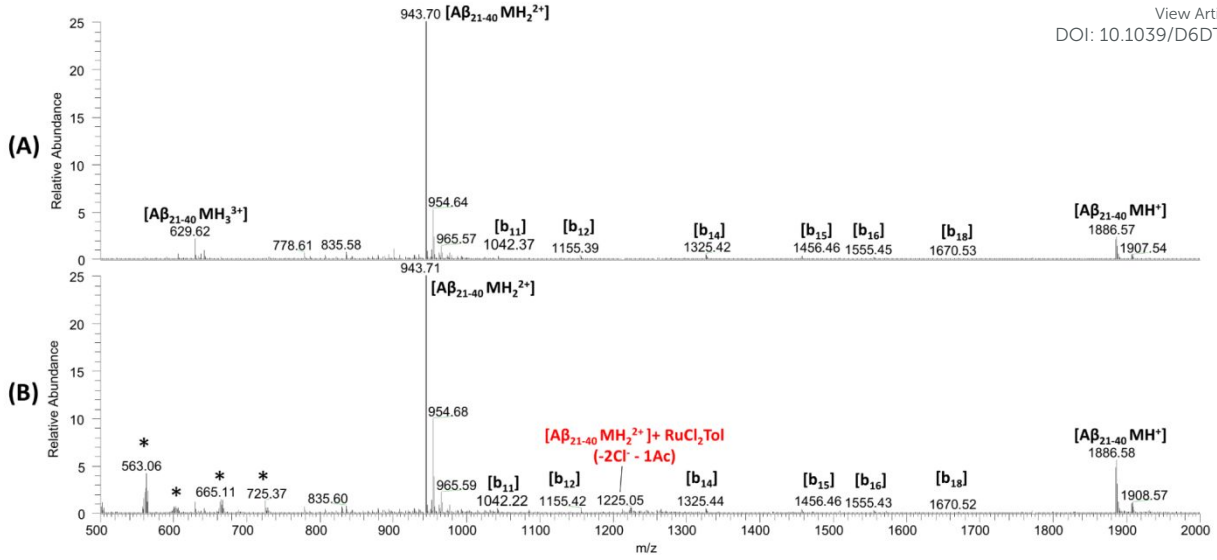

Figure 6. ESI-MS spectra of the $A\beta_{21–40}$ peptide in the absence (A) and presence of **$RuCl_2Tol$** (B). The peaks marked with bn derive from spontaneous source fragmentation of $A\beta_{21–40}$ (b series elements). Asterisks (*) highlight the species present in the control (**$RuCl_2Tol$** alone

Table 2: **Experimental m/z values detected in the spectra of $A\beta_{21-40}$ and $A\beta_{1-42}$ alone and with the addition of $RuCl_2Tol$**. The ion species corresponding to each experimental m/z, the expected m/z value (theoretical) and their charge states are also reported.

	Description	m/z (charge)		Theoretical m/z
		control	+ complex	
$A\beta_{1-42}$: **$RuCl_2Tol$**	$A\beta_{1-42}$	1505.35 (+3) 1129.15 (+4) 903.61 (+5) 753.28 (+6) 645.85 (+7)	1505.50 (+3) 1128.81 (+4) 903.57 (+5) 753.30 (+6) -	1505.71 1129.54 903.83 753.36 645.88
	b38	1371.78 (+3)	-	1371.34
	b34	1256.68 (+3)	1256.94 (+3)	1256.63
	$A\beta_{1-42}$ + **$RuCl_2Tol$** (-2Cl·, -2Ac)	-	1680.21 (+3) 1008.04 (+5) 840.17 (+6)	1679.91 1007.80 839.96
$A\beta_{21-40}$: **$RuCl_2Tol$**	$A\beta_{21-40}$	1886.57 (+1) 943.70 (+2) 629.62 (+3)	1886.58 (+1) 943.71 (+2) -	1886.19 943.60 629.40
	b18	1670.53 (+1)	1670.52 (+1)	1669.86
	b16	1555.45 (+1)	1555.43 (+1)	1555.81
	b15	1456.46 (+1)	1456.46 (+1)	1456.75
	b14	1325.42 (+1)	1325.44 (+1)	1325.71

View Article Online
DOI: 10.1039/D6DT00454G

	b12	1155.39 (+1)	1155.42 (+1)	1155.60
	b11	1042.37 (+1)	1042.22 (+1)	1042.52
	$A\beta_{21-40}$ + **$RuCl_2Tol$** (−2Cl^-, −1Ac)	-	1225.05 (+2)	1224.80

Effects of η⁶-Arene Ru(II) on the Aβ $_{1-42}$ cytotoxicity

MTT assay was performed to assess the potential protective effect of Ru complexes against $A\beta_{1-42}$ amyloid-induced cytotoxicity[29] at three different time points (0, 2 and 24 h) (Figure 7). As a preliminary step, the effects of Ru-complexes alone toward SH-SY5Y neuroblastoma cells were evaluated. Complexes did not show significant toxicity up to 24 h of incubation (Figure S4). As expected, treatment with $A\beta_{1-42}$ resulted in a significant, time-dependent reduction of cell viability (almost 20%), confirming its intrinsic neurotoxic effects [30]. The presence of the Ru-complexes determined different effects: both **$RuCl_2Tol$** and **RuPhenCym** exhibited a rescue of cell viability confirming that both complexes act as inhibitors of toxic aggregation. Conversely, **RuBipyCym**, consistently with its limited anti-aggregative activity, was unable to reduce the cytotoxicity induced by $A\beta_{1-42}$.

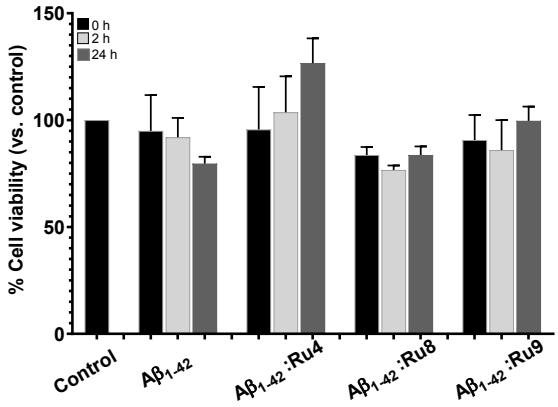

Figure 7. Effects of Ru-complexes on the cytotoxicity of Aβ1–42 peptides in SH-SY5Y neuroblastoma cells. Cell viability was evaluated by MTT assay after incubation of Aβ1–42 peptides in the absence or presence of Ru-complexes under stirring conditions at t = 0, 2, and 24 h. Control cells (untreated) were set as 100% viability. Data are presented as mean ± standard deviation (SD) from three independent experiments. Statistical analysis was performed using one-way ANOVA followed by Dunnett's multiple comparisons test, comparing all treatment groups to the control condition. No statistically significant differences were observed.

Experimental

Peptides and metal complexes syntheses

$A\beta_{1-42}$ and $A\beta_{21-40}$ were purchased from NovoPro Bioscience Inc. (Shanghai, China). All peptides were treated with 1,1,1,3,3,3-hexafluoro-2-propanol (HFIP) to guarantee a monomeric state, lyophilized and stored at -20 °C until use.

Ru complexes were synthetized as reported in [27].

Fluorescence Assays

ThT emission assays were carried out in black plates (96 well) under stirring on fluorescence reader Envision 2105 (Perkin Elmer). Measurements were collected every 7 min (λ_{ex} 440 nm and λ_{em} 483 nm). Assays were performed in duplicate at 25 °C employing a peptide concentration of 100 µM for $A\beta_{21-40}$, and 50 µM for $A\beta_{1-42}$ in 50 mM NaCl and 20 mM phosphate buffer (pH 7.4), using a ThT final concentration of 50 µM for $A\beta_{21-40}$, and 5 µM for $A\beta_{1-42}$. Different ThT concentrations were employed to ensure optimal signal-to-noise ratios for each peptide system. Different ratios with metal complexes (stock solutions 2 mM in water) were tested.

Circular Dichroism (CD) Spectroscopy

CD spectra of $A\beta_{1-42}$ at 50 µM and $A\beta_{21-40}$ at 100 µM, in 10 mM phosphate buffer pH 7.4, in the absence and presence of the metal compounds in 1:1 peptide to complex molar ratio, were registered on a Jasco J-815 spectropolarimeter (JASCO, Tokyo, Japan), at 25 °C using a 0.1 cm path-length quartz cuvette. CD spectra were recorded overtime using solutions prepared by the dilution of freshly prepared stock solutions of Aβ peptides (~1 mM) [31]. Deconvolutions of CD spectra were obtained by BESTSEL software (http://bestsel.elte.hu/)[32]

ESI-MS

The solution of $A\beta_{21-40}$ or $A\beta_{1-42}$ at a concentration of 50 µM in 15 mM ammonium acetate (AMAC) buffer at pH = 7.0 was incubated with metal compounds in a peptide to metal compound molar ratio of 1 : 1. The solutions were diluted 10 times with 15 mM AMAC and then analyzed using a LTQ XL ion trap mass spectrometer equipped with an electrospray ionization (ESI) source operating at a needle voltage of 3.5 kV and 320 °C with a complete Ultimate 3000 HPLC system, including a pump MS, an autosampler, and a photodiode array (all from Thermo Fisher Scientific). Spectra of the isolated peptides and the three complexes alone were recorded as controls.

SEM analysis

$A\beta_{1-42}$ (50 µM) and $A\beta_{21-40}$ (100 µM) alone and in the presence of Ru-complexes (1: 1 peptide: complex molar ratio) in 10 mM phosphate buffer, pH 7.4, were morphologically analyzed after 6 h of aggregation using field-emission SEM (Phenom_XL, Alfatest, Milan, Italy). After this time, ~30 µL of solution was drop-cast on an aluminum stub and vacuum dried to prepare each sample. For 75 s, a thin layer of gold was sputtered at a current of 25 mA. The sputter-coated samples were then introduced into the microscope chamber,

View Article Online
DOI: 10.1039/D5DT00454G

and micrographs were acquired with a secondary electron detector (SED) operating at an accelerating voltage of 10 kV. The Ru-complexes and buffer alone (Figure S5) were analyzed as controls

Cell Culture

SH-SY5Y human neuroblastoma cells (CRL-2266; ATCC, Manassas, VA, USA) were grown in 100 × 20 mm culture dishes at a density of 1 × 10^6 cells per dish. Cells were maintained in DMEM (Corning; Cat. No. 10–013-CV) supplemented with 10% fetal bovine serum (Sial; Cat. No. YourSIAL-FBS-SA), 100 U mL^{-1} penicillin, 100 µg mL^{-1} streptomycin (Corning; Cat. No. 30–002-CI), and 25 mM HEPES (Sigma-Aldrich; Cat. No. H0887). Cultures were incubated at 37 °C in a humidified environment containing 5% CO_2 and were subcultured when approximately 80% confluence was reached.

MTT Assay.

$A\beta_{1–42}$ (stock solution 100 µM in 50 mM phosphate buffer at pH 7.4) in the absence and in the presence of the Ru-complexes at a 1:1 peptide to metal complex molar ratio (after 0, 2 and 24 h of stirring) were diluted in a cell culture medium at a final concentration of 25 µM and added to the cells for 24 h. Prior to cell treatment, samples were visually inspected to exclude precipitation. No visible aggregation or precipitation was observed under the experimental conditions. Control cells were incubated with phosphate buffer diluted in the cell culture medium at the same final concentration used for the peptide. Following treatment, cell viability was assessed using the MTT assay according to the manufacturer's protocol. Briefly, 100 µL of MTT solution (final concentration 0.5 mg/mL; Sigma-Aldrich) was added to each well and incubated for 2 h. The medium was then removed, and DMSO was added to dissolve the formazan crystals generated by metabolically active cells. Absorbance was measured at 570 nm using a microplate reader (VICTOR Nivo™, Revvity). A background absorbance value of 0.2, determined from cell-free wells treated with MTT, was subtracted from all readings. Cell viability was calculated by normalizing the mean absorbance values of cells treated with $A\beta_{1-42}$, in the absence or presence of Ru-complexes, to those of buffer-treated control cells and expressed as a percentage of control. In addition, the intrinsic cytotoxic effects of the Ru complexes were independently evaluated.

Conclusion

The binding of Ru (II) complexes to Aβ peptides is highly tuned by the nature of ligands in the coordination sphere: charge, aromaticity, chelate state[24, 30, 33]. This study demonstrates that η^6-arene Ru(II) complexes can effectively modulate amyloid-β aggregation and proposed mechanisms are highly dependent on peptide length, composition and ligand fields. Among the investigated compounds, **RuPhenCym** and **$RuCl_2$Tol** emerged as the most active species, displaying complementary modes of action. **RuPhenCym** predominantly interferes with $A\beta_{1–42}$ aggregation via aromatic and supramolecular interactions, leading to the stabilization of soluble β-sheet–containing species and a pronounced reduction of fibril growth. The presence of soluble β-structured species is inferred from spectroscopic data but cannot be conclusively established without complementary size-distribution techniques such as DLS or SEC. In contrast, **$RuCl_2$Tol**, characterized by a more labile coordination sphere, forms stable peptide adducts via coordination mechanism and efficiently disrupts aggregation of both $A\beta_{1–42}$ and $A\beta_{21–40}$. While these observations are consistent with distinct coordination- versus supramolecular-driven mechanisms, definitive identification of binding sites and aggregate nature will require further structural investigations. Non-covalent interactions are proposed based on indirect evidence, and further studies (e.g., NMR or computational modeling) will be required to identify specific binding sites. The ability of **$RuCl_2$Tol** and **RuPhenCym** to significantly rescue $A\beta_{1–42}$–induced cytotoxicity in neuronal cells establishes a direct link between the modulation of aggregation pathways and biological outcome, underscoring the relevance of metal-mediated control of amyloid assembly for mitigating neurotoxicity. Importantly, the lack of intrinsic cellular toxicity of the Ru complexes under the investigated conditions further supports their suitability as potential neurodrugs. Collectively, these results highlight η^6-arene Ru(II) complexes as versatile platforms for the development of metal-based agents targeting pathological amyloid aggregation. The tunability of ligand frameworks and coordination lability enables selective engagement with toxic amyloid species, offering a rational foundation for the design of next-generation bioinorganic modulators with potential theranostic relevance in neurodegenerative disorders associated with amyloid misfolding.

Author Contributions

Funding acquisition, Conceptualization, Original Draft: D.M., Supervision, Review & Editing D.M. and S. L. M; Investigation and formal analysis: S. L. M., C. D S.,D.F., F.R., A. A.

Conflicts of interest

There are no conflicts to declare.

Data availability

The data supporting this article have been included as part of the Supplementary Information.

Founding source

This work was supported by #NEXTGENERATIONEU (NGEU), Ministry of University and Research (MUR), National Recovery and Resilience Plan (NRRP), project MNESYS (PE0000006) – A Multiscale integrated approach to the study of the nervous system in health and disease (DN. 1553 11.10.2022).

ACKNOWLEDGMENT

D.F. acknowledge the Italian Ministry of Health– Ricerca Corrente Project.

Notes and references

1. M. Oprica, E. Hjorth, S. Spulber, B. Popescu, M. Ankarcrona, B. Winblad and M. Schultzberg, *Journal of Cellular and Molecular Medicine*, 2007, **11**, 810-825.
2. S. La Manna, C. Di Natale, V. Panzetta, P. A. Netti, A. Merlino, K. Kowalski and D. Marasco, *Inorganic Chemistry Frontiers*, 2024, **11**, 6577-6587.
3. A. Baumketner, S. L. Bernstein, T. Wyttenbach, N. D. Lazo, D. B. Teplow, M. T. Bowers and J. E. Shea, *Protein science*, 2006, **15**, 1239-1247.
4. S. La Manna, C. Di Natale, V. Panzetta, M. Leone, F. A. Mercurio, I. Cipollone, M. Monti, P. A. Netti, G. Ferraro and A. Terán, *Inorganic Chemistry*, 2023, **63**, 564-575.
5. G. Leech, A. L. Acosta, S. Mahato, P. C. Barrett, R. O. Hodges, S. A. McFarland and T. Storr, *Chemical Science*, 2025, **16**, 20914-20923.
6. Y.-B. Peng, C. Tao, C.-P. Tan and P. Zhao, *Journal of Inorganic Biochemistry*, 2021, **224**, 111591.
7. N. A. Vyas, S. N. Ramteke, A. S. Kumbhar, P. P. Kulkarni, V. Jani, U. B. Sonawane, R. R. Joshi, B. Joshi and A. Erxleben, *European Journal of Medicinal Chemistry*, 2016, **121**, 793-802.
8. S. Singh, G. R. Navale, S. Agrawal, H. K. Singh, L. Singla, D. Sarkar, M. Sarma, A. R. Choudhury and K. Ghosh, *International journal of biological macromolecules*, 2023, **239**, 124197.
9. R. M. Hacker, D. M. Grimard, K. A. Morgan, E. Saleh, M. M. Wrublik, C. J. Meiss, C. C. Kant, M. A. Jones, W. W. Brennessel and M. I. Webb, *Dalton Transactions*, 2024, **53**, 18845-18855.
10. J. C. Bataglioli, L. M. Gomes, C. Maunoir, J. R. Smith, H. D. Cole, J. McCain, T. Sainuddin, C. G. Cameron, S. A. McFarland and T. Storr, *Chemical Science*, 2021, **12**, 7510-7520.
11. G. Leech, A. L. Acosta, S. Mahato, P. C. Barrett, R. O. Hodges, S. A. McFarland and T. Storr, *Chemical Science*, 2025.
12. D. Florio, M. Cuomo, I. Iacobucci, G. Ferraro, A. M. Mansour, M. Monti, A. Merlino and D. Marasco, *Pharmaceuticals (Basel)*, 2020, **13**.
13. G. K. Yawson, S. E. Huffman, S. S. Fisher, P. J. Bothwell, D. C. Platt, M. A. Jones, G. M. Ferrence, C. G. Hamaker and M. I. Webb, *Journal of inorganic biochemistry*, 2021, **214**, 111303.
14. G. Son, B. I. Lee, Y. J. Chung and C. B. Park, *Acta biomaterialia*, 2018, **67**, 147-155.
15. G. K. Yawson, M. F. Will, S. E. Huffman, E. T. Strandquist, P. J. Bothwell, E. B. Oliver, C. F. Apuzzo, D. C. Platt, C. S. Weitzel and M. A. Jones, *Inorganic Chemistry*, 2022, **61**, 2733-2744.
16. J.-M. Suh, G. Kim, J. Kang and M. H. Lim, *Journal*, 2018, **58**, 8-17.
17. D. Florio, A. Annunziata, V. Panzetta, P. A. Netti, F. Ruffo and D. Marasco, *Inorganic Chemistry*, 2024, **63**, 16001-16010.
18. A. De Santis, S. La Manna, I. R. Krauss, A. M. Malfitano, E. Novellino, L. Federici, A. De Cola, A. Di Matteo, G. D'Errico and D. Marasco, *Biochimica et Biophysica Acta - General Subjects*, 2018, **1862**, 967-978.
19. S. La Manna, P. L. Scognamiglio, V. Roviello, F. Borbone, D. Florio, C. Di Natale, A. Bigi, C. Cecchi, R. Cascella, C. Giannini, T. Sibillano, E. Novellino and D. Marasco, *FEBS J*, 2019, **286**, 2311-2328.
20. K. L. Morris, A. Rodger, M. R. Hicks, M. Debulpaep, J. Schymkowitz, F. Rousseau and L. C. Serpell, *Biochemical Journal*, 2013, **450**, 275-283.
21. Z. S. Al-Garawi, K. L. Morris, K. E. Marshall, J. Eichler and L. C. Serpell, *Interface Focus*, 2017, **7**, 20170027.
22. D. Florio, S. La Manna, A. Annunziata, I. Iacobucci, V. Monaco, C. Di Natale, V. Mollo, F. Ruffo, M. Monti and D. Marasco, *Dalton Transactions*, 2023, **52**, 8549-8557.
23. F. Bossis and L. L. Palese, *Biochimica et Biophysica Acta (BBA)-Proteins and Proteomics*, 2013, **1834**, 2486-2493.
24. S. La Manna, C. Di Natale, V. Panzetta, M. Leone, F. A. Mercurio, I. Cipollone, M. Monti, P. A. Netti, G. Ferraro, A. Teran, A. E. Sanchez-Pelaez, S. Herrero, A. Merlino and D. Marasco, *Inorg Chem*, 2024, **63**, 564-575.
25. S. La Manna, D. Florio, J. A. Platts, E. Gabano, M. Ravera and D. Marasco, *Dalton Transactions*, 2025, **54**, 10416-10425.
26. S. La Manna, M. Leone, I. Iacobucci, A. Annuziata, C. Di Natale, E. Lagreca, A. M. Malfitano, F. Ruffo, A. Merlino and M. Monti, *Inorganic Chemistry*, 2022, **61**, 3540-3552.
27. A. Annunziata, M. E. Cucciolito, M. Di Ronza, G. Ferraro, M. Hadiji, A. Merlino, D. Ortiz, R. Scopelliti, F. Fadaei Tirani and P. J. Dyson, *Organometallics*, 2023, **42**, 952-964.
28. S. L. Manna, D. Florio, I. Iacobucci, F. Napolitano, I. D. Benedictis, A. M. Malfitano, M. Monti, M. Ravera, E. Gabano and D. Marasco, *International journal of molecular sciences*, 2021, **22**, 3015.
29. D. A. Butterfield and D. Boyd-Kimball, *Brain Pathology*, 2004, **14**, 426-432.
30. S. La Manna, V. Panzetta, C. Di Natale, I. Cipollone, M. Monti, P. A. Netti, A. Terán, A. E. Sánchez-Peláez, S. Herrero and A. Merlino, *Inorganic Chemistry*, 2024, **63**, 10001-10010.
31. B. Tizzano, P. Palladino, A. De Capua, D. Marasco, F. Rossi, E. Benedetti, C. Pedone, R. Ragone and M. Ruvo, *Proteins: Structure, Function, and Bioinformatics*, 2005, **59**, 72-79.
32. A. Micsonai, F. Wien, L. Kernya, Y.-H. Lee, Y. Goto, M. Réfrégiers and J. Kardos, *Proceedings of the National Academy of Sciences*, 2015, **112**, E3095-E3103.
33. S. La Manna, C. Di Natale, V. Panzetta, M. Leone, F. A. Mercurio, I. Cipollone, M. Monti, P. A. Netti, G. Ferraro, A. Terán, A. E. Sánchez-Peláez, S. Herrero, A. Merlino and D. Marasco, *Inorganic Chemistry*, 2024, **63**, 564-575.

Data availability statement (DAS)

View Article Online
DOI: 10.1039/D6DT00454G

The data supporting this article have been included as part of the Supplementary Information